



# MECHANISMS AND APPLICATIONS OF CATALYTIC COMBUSTION OF NATURAL GAS\*

Shihong Zhang<sup>#</sup>, Ning Li, Zhihua Wang

*Beijing University of Civil Engineering and Arch., Beijing, China*

## ABSTRACT

This article discussed the thermal efficiency, stability and pollutant emissions characteristics of the combustion of lean natural gas-air mixtures in Pd metal based honeycomb monoliths by means of experiments on a practical burner V. The chemistry at work in the monoliths was then investigated by the stagnation point flow reactor (SPFR), a fundamental experimental reactor. It was found that catalytic combustion inhibited the extent of gas-phase oxidation and increased the surface temperature of homogeneous ignition. According to the applications of catalytic combustion in the condenser boiler, the data of catalytic combustion condenser boiler V were measured at atmospheric temperature and pressure. The study also showed that more than 95% of its thermal efficiency was found possible while preserving near zero pollutant emissions. For all the catalysts tested, flow rates, and mixture compositions of natural gas and air used here, neither CO (the unburned fuel) nor NO<sub>x</sub> were detected as long as surface combustion was taking place.

**Keywords:** *Catalytic combustion; Condenser boiler; Thermal efficiency.*

## 1. INTRODUCTION

A catalyst is a 'substance that speeds up a chemical reaction without itself undergoing any permanent chemical change. The study of catalysis is a huge subject which covers many disciplines from biological sciences to mathematical modeling. Catalytically stabilized thermal combustion (CST) has received increased interest for its potential to expand the lean stability limit and achieve ultra low emissions in practical combustors such as stationary gas turbines, industrial boilers or household burners (Dogwiler and Benz *et al.*, 1999). There are complex interactions between heterogeneous and homogeneous oxidation reactions at intermediate temperature. The low concentrations of fuel near the surface are caused by synergetic gas-phase and surface chemistry effects (Vlachos, 1996). The chemistry at work in the monoliths was investigated using fundamental experimental reactors including SPFR (Taylor and Allendorf *et al.*, 2003). It was found that catalytic combustion inhibited the extent of gas-phase oxidation and increased the surface temperature of homogeneous ignition. This proved that catalytic combustion could be used in high-temperature environments.

Low pollution emissions and high thermal efficiency are most important for boiler. Catalytic combustion of natural gas just has these advantages. The oxidation reaction of heterogeneous catalytic combustion is almost complete. There are almost no products of incomplete combustion from catalytic combustion such as CnHm and CO. And its combustion efficiency almost achieves 99.9%. Catalytic combustion can achieve the dual objective of energy-saving and emission reduction.

At present, the research in catalytic combustion technology was mainly related to its applications in domestic water heater, combustors of stationary gas turbines for power generation and heating purposes (Seonhi *et al.*, 1997; Scholten *et al.*, 1999; Kang *et al.*, 1999). In our article, the applications of catalytic combustion were concerned. It included the thermal efficiency of catalytic combustion boiler, the surface temperature of catalytic burner and the combustion characteristic of catalyst.

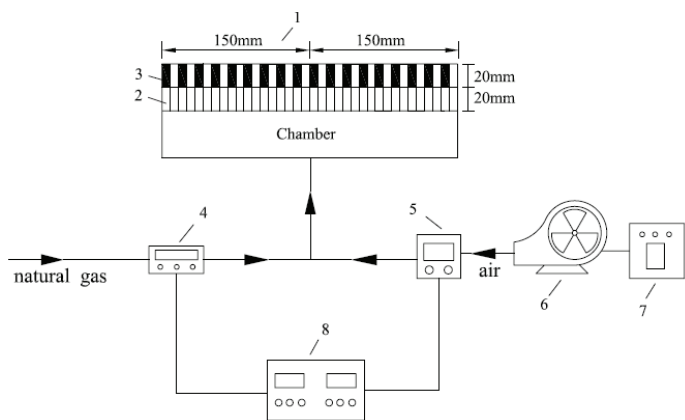
## 2. EXPERIMENTAL SET-UP

Figure 1 illustrates the catalytic combustion burner V. The square honeycomb monoliths were 150mm wide in sides of the square and 20mm long, with square-shaped cells which sectional area was 1mm×1mm. The support for all the monoliths tested here was cordierite. The two square catalytic honeycomb monoliths were installed in the burner-V each time.

As the reaction zone inside the catalysts was ended at about 10mm from the monolith's entrance, so the lengths of catalytic honeycomb monoliths were reduced to 20mm for the catalytic combustion burner. In order to decrease the temperature of mixtures in chamber connected with the monolith's entrance, the 20mm long blank monoliths were inserted between the chamber and the Pd based catalytic monolith's entrance as assembly of monolith.

\* Presented at the 14th International Heat Transfer Conference, Washington, DC, August 8-13, 2010. Republished with permission from American Society of Mechanical Engineers (ASME).

<sup>#</sup> Corresponding author. Email: [shihongzhang@bucea.edu.cn](mailto:shihongzhang@bucea.edu.cn).



**Fig. 1** Combustion system of catalytic combustion burner V (1. catalytic burner 2. blank monoliths 3. catalytic monoliths 4. mass flow CGS 5. gas-flow monitor CGM 6. fan 7. micromaster420 8. Manostat)

The reactant gas feeds of natural gas and air were regulated via GMS0050BSRN200000 natural gas meter and CMG400A080100000 air meter with 0~50 L/min and 0~80m<sup>3</sup>/h of full-scale ranges, respectively. As shown in Figure 2, the surface of the two monoliths was divided into eighteen uniform regions with the sectional area of 50mm×50mm. The local surface temperature of catalytic monolith was measured by UX-20P infrared radiation thermometer with 600~3000□ of full-scale ranges.

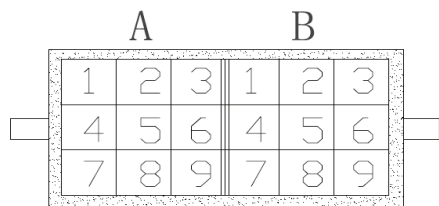


**Fig. 2** Surface of the two monoliths

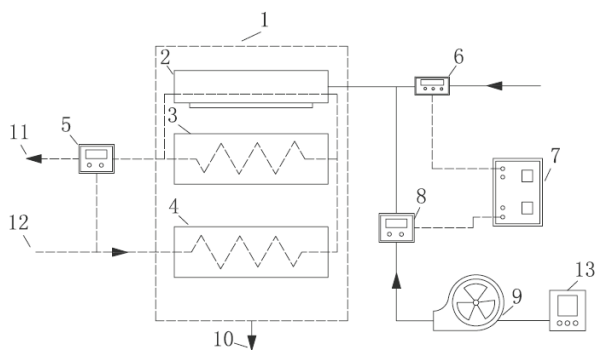


**Fig. 3** System of catalytic combustion condenser boiler V (1. boiler casing 2. catalytic burner 3. first stage heat exchanger 4. second stage heat exchanger, 5. multi cumulative heat meter (WFP-21) 6. mass flow CGS 7. manostat 8. gas-flow monitor CGM 9. fan 10. condensate 11. water outlet 12. water inlet 13. micromaster 420)

Figure 3 illustrates the system of catalytic combustion condensing boiler V. This system had two heat exchangers. The radiation heat transfer was absorbed by first stage heat exchanger which was close to the catalytic burner, and the convection heat transfer was absorbed by second stage heat exchanger. Water firstly went into the second stage heat exchanger, and then entered the first stage heat exchanger and

catalytic burner respectively. At last hot water was drained away from the water outlet.

The multi cumulative heat meter with 20~90°C of full-scale ranges for the parameters of water. A measuring cylinder for the condensation of vapor were used. And the exhaust gas temperature at open end of monolith was measured by thermocouple K of diameter 0.5. The each experiment was run for 1 hour.

### 3. EXPERIMENTAL RESULT AND DISCUSSION

#### 3.1 Mechanism of catalytic combustion of methane

The emissions characteristics of the combustion of fuel-lean mixtures of natural gas and air were studied in steady-state conditions in a catalytic honeycomb monolith burner. In order to investigate the parameters controlling the kinetics and products selectivities of the heterogeneous (solid-gas) oxidation of methane (main composition of natural gas) on a ‘model’ noble metal, and the homogeneous ignition inhibition phenomenon, fundamental work on a small-scale reactor was carried out (the stagnation point flow reactor or SPFR). The combustion of lean CH<sub>4</sub>/O<sub>2</sub>/N<sub>2</sub> mixtures on a polycrystalline platinum foil in a stagnation point flow reactor at atmospheric pressure and in steady-state was investigated. The Experimental set-up was the same as that of the work (Dupont *et al.*, 2002). The following equations (1) and (2) for the percent fuel conversion CV<sub>CH<sub>4</sub></sub> and the selectivity of products SEL<sub>k</sub> for the species ‘k’ were derived (on a mol basis):

$$CV_{CH_4} = -100 \frac{F_{CH_4} C_S + \int_0^L W_{CH_4} \dot{\omega}_{CH_4} C dx}{\rho_0 Y_{CH_4,0} U_0} \quad (1)$$

$$SEL_k = -100 \frac{\frac{F_k}{W_k} C_S + \int_0^L \dot{\omega}_k C dx}{[ \frac{F_{CH_4}}{W_{CH_4}} C_S ] + \int_0^L \dot{\omega}_{CH_4} C dx} \quad (2)$$

where  $W_k$  is the molar mass of the species k,  $\dot{\omega}_k$  (in mol/ cm<sup>3</sup> · s), is the molar production rate of k,  $F_k$  (in kg/ cm<sup>2</sup> · s), is the mass flux of k at the foil surface, the subscript 0 means ‘at the injector outlet’ (x = 0 cm).  $\rho_0$ ,  $Y_{CH_4,0}$ , and  $U_0$  are the gas density, fuel mass fraction and axial velocity at the injector outlet, their product being the mass flux of fuel in the reactor. The coefficient C is a correction factor which accounts for a slight radial expansion of the control volume used to perform the species balances in the calculation of the fuel conversion and products selectivities.. This control volume, originally cylindrical with a radius r at its basis (location of injector) increasing to a radius  $r_s^* = r(1 + KLT_s/T_j)$  at the catalytic surface. Cs corresponds to x = L = 1cm, i.e, the value of C at the foil surface. For our SPFR, we show the conversion curves obtained this time without correction factor, therefore it is one. The proportionality constant K was chosen to match the predicted fuel conversion of a sample point with its corresponding experimental value.

In order to describe the foil condition for each experiment, two parameters were varied in order to investigate their effects on the fuel conversions and CO selectivities; these are:

1. The fuel mixture strength by varying the parameter  $\alpha =$

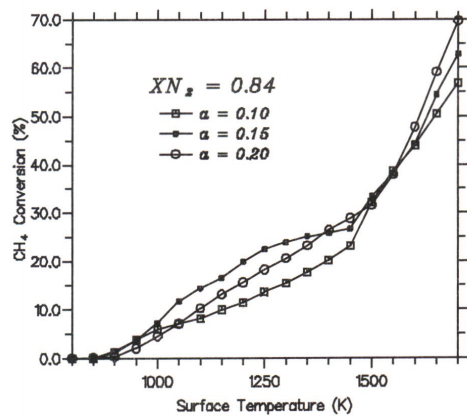
$\dot{V}_{CH_4} / (\dot{V}_{CH_4} + \dot{V}_{O_2})$ , where  $\dot{V}_k$  is the input volume flow rate of the relevant species k,  $\alpha$  was varied from 0.1 to 0.3, with stoichiometry at 1/3.

2. The N<sub>2</sub> the mol fraction of nitrogen gas in the inlet mixture,

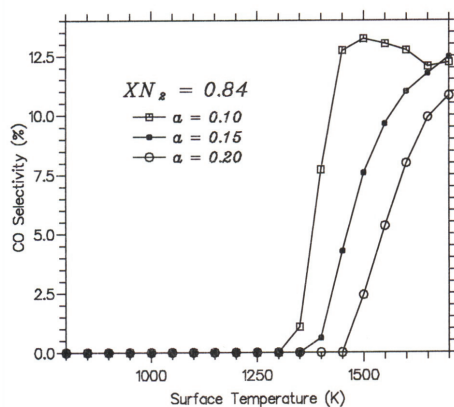
$$X_{N_2} = (\dot{V}_{N_2} + 0.79 \dot{V}_{air}) / \dot{V}_{tot}, \text{ (from 0.791 to 0.874).}$$

Figure 4(a). (b) show the CH<sub>4</sub> conversions and CO selectivities for the three ultra-lean values of  $\alpha$  (0.1, 0.15, and 0.2) and XN<sub>2</sub> (0.84) .

The stagnation point flow option from the program SPIN solves the finite difference approximations of the species, momentum and energy conservation equations on the symmetry axis of the reactor using a hybrid Newton/time-step algorithm. The fast solution method used in SPIN permitted testing detailed chemical kinetic mechanisms as well as global reaction mechanisms. The global reaction mechanism attributed a clear catalytic role to the Pt surface over all the fuel conversion regimes. The gas phase conversion started at a surface temperature 1200 K without the catalyst according to the work (Dupont *et al.*, 2001).



(a)



(b)

**Fig. 4** CH<sub>4</sub> conversion and CO selectivity dependence on Pt catalyst temperature. ( $U_0=4.5-4.6$  cm/s)

The investigation showed that the gas-phase fuel/air mixture did not ignite until the temperature at the catalytic surface was significantly above the ordinary auto-ignition temperature. From figure 4(a),(b) the gas phase ignition was about 1400-1500 K. This inhibition of gas-phase combustion by the catalytic reactions is desirable, since it extends the range over which clean and stable oxidation conditions persist. For all tested in the catalytic honeycomb monolith burner V, neither CO (the unburned fuel) nor NO<sub>x</sub> were detected as long as surface combustion was taking place.

### 3.2 Temperature

Figure 5 plots average local surface temperature of monolith and average gas temperature at the open end of monolith between 4 and 13.09 kW in thermal input of catalytic burner. As we can see from the profiles, average local surface temperature and average gas temperature ascended gradually with the increasing thermal input firstly, then their temperature began to decrease when the thermal input reached 12 kW. The combustion was stable between 4 kW and 12 kW. But a part area of catalyst became black gradually at 13.09 kW. The highest surface

temperature among all the areas was measured to be 1180° when the thermal input was 12 kW.

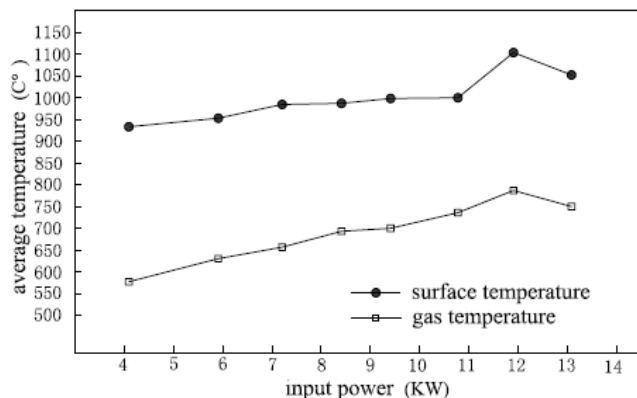


**Fig. 5** Curves of average local surface temperature of monolith and average gas temperature at open end of monolith

### 3.3 Condensate

The exhaust gases contained large amounts of vapor. The available latent heat in the exhaust gases is directly proportional to the amount of vapor. In the condition of same thermal input, the boiler thermal efficiency was enhanced with the increase of condensate volume per unit time. Therefore, condensate was important to increase the boiler's thermal efficiency. Its heat transfer process is very complex, which is influenced by many factors, such as excess air ratio, exhaust gas flow rate and perturbation effect. Under the conditions of thermal input and variable water flow rate, the condensate and its efficiency of catalytic combustion condensing boiler V were measured respectively.

Because a little composition of vapor in the air have been ignored for calculation of condensate volume in productions, calculated condensate volume  $V$ (ml), was produced from the combustion of methane (main composition of natural gas) by the formula(3):

$$V = 10^6 \frac{M_{rH_2O} V_{vapor} V_g}{\rho_{H_2O} V_m} \quad (3)$$

where  $M_{rH_2O}$  is the molar mass of water molecules (g/mol), and  $V_g$  is the volume of nature gas, ( $Nm^3$ ). is the volume of vapor generated from the burning of a standard volume of nature gas, where  $V_{vapor}=2 \times 0.96=1.92Nm^3$ , 0.96 is percent of methane in nature gas mixture and the volume of vapor(supposed as ideas gas) is  $2 Nm^3$  under standard conditions generated from  $1Nm^3$  methane.  $V_m$  is molar volume, where it is 22.4L/mol.  $\rho_{H_2O}$  is the density of water, where it is  $1.0 \times 10^3 kg/m^3$ . Figure 6 shows condensate volume and condensation efficiency.

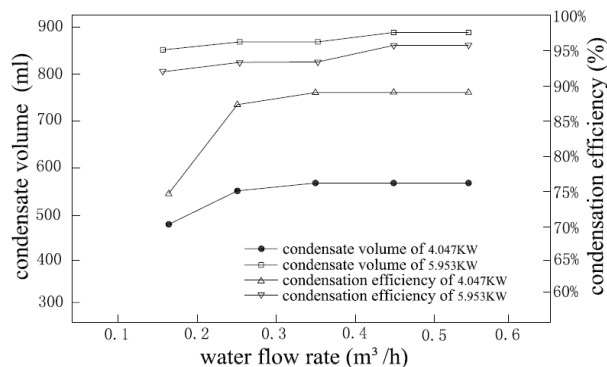


**Fig. 6** Curves of condensate volume and the corresponding condensation efficiency vs water flow rate.

The condensate volume increased firstly, then was steady with increasing water flow rate. The maximum difference of condensate

volume between 5.953 kW and 4.047 kW was 340 ml which was caused by a rise of thermal input. The highest condensation efficiency reached 96.39% in this experiment. It was seen that the condensation efficiency of 5.953 kW was higher than that of 4.047 kW.

### 3.4 Thermal efficiency

In order to study thermal efficiency of catalytic combustion condensing boiler V the experiment was carried out by different water volume into the heat exchanges with two input power. The thermal efficiency of boiler was calculated by equation (4):

$$\eta = Q_i / Q_r = 60GC_m(t_0 - t_i) / H_h L_g \quad (4)$$

where  $Q_i$  is the thermal output of catalytic combustion boiler, kW. Similarly,  $Q_r$  is the thermal input of catalytic combustion boiler, kW.  $G$  is mass flow rate, kg/s.  $C_m$  is specific heat of water, which was equal to 4187J/(kg.°C) here.  $t_0$  and  $t_i$  are water outlet and inlet temperature respectively. And  $L_g$  is the amount of gas consumed, L/min.  $H_h$  is gross calorific value of natural gas under standard conditions, which was  $H_h = 39.584 \text{ MJ/Nm}^3$ .

In this experiment, the thermal inputs were 4.047 kW and 5.953 kW respectively, as shown in figure 7, the thermal efficiency of catalytic combustion condenser boiler V was more than 93% according to equation (4).

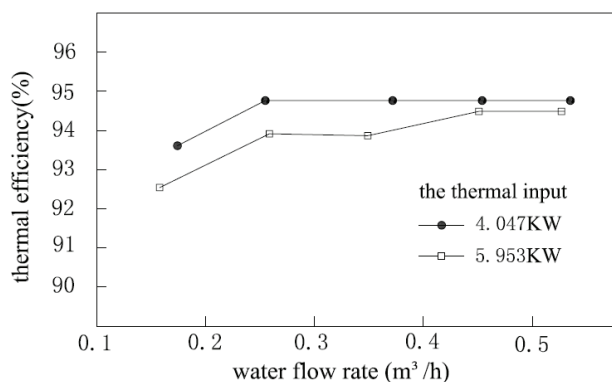


Fig. 7 Curves of the thermal efficiency with respect to water flow rate.

The thermal efficiency of 4.047 kW was higher than that of 5.953 kW because there was big thermal loss with the increase of thermal input, such as the heat loss of boiler outer casing, exhaust gas and so on. The boiler's thermal efficiency was increased quickly, then was steady with the increase of water flow rate. Temperature of exhaust gas also had a small decrease with the increase of water flow rate. When the water flow rate was enhanced, the average temperature of pipe wall was decreased which lead to a rise of condensate volume.

Under the conditions of small input power and big water flow rate, the maximum of thermal efficiency in catalytic combustion condensing boiler V reached about 94.74%. And the exhaust gas temperature was about 12°C, which was lower than the room temperature and close to the temperature of input water  $t_i$  which was about 10°C in the experiment.

The thermal output  $Q_i$  was obtained by multi cumulative heat meter (WFP-21) as shown in figure 3. It was run for 5 different water flow rates with the thermal input of 4.047 kW and 5.953 kW, respectively. The period was 1 hour for each run.

From the psychrometric chart of an atmospheric pressure by atmospheric temperature (dry bulb temperature) and air humidity ratio, the exhaust gas temperature was reduced to near the dew point of the air. It proved that the condensation efficiency was very high.

## 4. CONCLUSIONS

The radiation fluxes of catalytic burner were higher because of high surface temperature of catalytic monolith. A specially designed heat exchangers were suitable for catalytic combustion. Also its condensation efficiency was very high. It is found that the content of  $C_nH_m$  and CO were closed to zero and thermal energy of natural gas could be used completely. High thermal efficiency and 'near' zero pollution emissions of catalytic combustion condenser boiler-V were the dual advantages of energy-saving and environmental protection which would be applied for industry.

## ACKNOWLEDGMENT

The project sponsored by the Beijing Municipality Key Lab of Heating, Gas Supply, Ventilating and Air Conditioning Engineering (KF201002); funding project for Academic Human Resources Development in Institutions of Higher Learning of Beijing Municipality (PHR201007127) and 2010 funding project (Building environment and facilities engineering).

## NOMENCLATURE

$C$	correction factor
$C_m$	specific heat of water J/(kg•°C)
$CV$	fuel conversion (%)
$F_k$	mass flux of k at the foil surface, (kg/ cm <sup>2</sup> •s)
$G$	mass flow rate (kg/s)
$H_h$	gross calorific value (MJ/Nm <sup>3</sup> )
$L_g$	gas volum (m <sup>3</sup> )
$M_{rH_2O}$	molar mass of water (g/mol)
$Q_i$	thermal output ( kW)
$SEL_K$	selectivity of products for the species 'k'
$U_0$	axial velocity 'at the injector outlet' (x = 0 cm ), (m/s)
$V_g$	volume of nature gas (Nm <sup>3</sup> )
$\dot{V}_k$	input volume flow rate of the relevant species k
$Y_{CH_4, 0}$	fuel mass fraction 'at the injector outlet' (x = 0 cm )
$W_k$	molar mass of the species k

### Greek Symbols

$\rho_0$	gas density at the injector outlet' (x = 0 cm ), (kg/m <sup>3</sup> )
$\eta$	thermal efficiency (%)
$\dot{\omega}_k$	molar production rate of k (mol/ cm <sup>3</sup> •s)

## REFERENCES

- Dogwiler, U., Benz P., Mantzaras, J., 1999, "Two-Dimensional Modelling For Catalytically Stabilized Combustion of a Lean Methane-Air Mixture with Elementary Homogeneous and Heterogeneous Chemical Reactions", *Combustion and Flame*, 116: 243-258  
[http://dx.doi.org/10.1016/S0010-2180\(98\)00036-4](http://dx.doi.org/10.1016/S0010-2180(98)00036-4)
- Dupont, V., Zhang, S. H., Williams, A., 2001, "Experiments and simulations of methane oxidation on a platinum surface", *Chemical Engineering Science*, 56 (8): 2659-2670  
[http://dx.doi.org/10.1016/S0009-2509\(00\)00536-4](http://dx.doi.org/10.1016/S0009-2509(00)00536-4)
- Dupont, V., Zhang, S. H., Williams, A., 2002, "High-Temperature catalytic combustion and its inhibition of gas-phase ignition", *Energy & Fuels*(16), 1576-1584  
<http://dx.doi.org/10.1021/ef020125k>
- Kang, S. K., Jeong, N. J., Ryu, I. S., Baek, Y. S., 1999, "Combustion control-technologies of catalytic burner applying to reduction-induced

furnace”, The 4th International Workshop on Catalytic Combustion, San Diego, April, 14-16

Scholten, A., van Yperen, R., Emmerzaal, I. J., 1999, “ A zero NOx catalytic ceramic natural gas cooker”, The 4th International Workshop on Catalytic Combustion, San Diego, April, 14-16

Seonhi, R., Scholten, A., 1997, “Comparison of catalytic and catalytically stabilized domestic natural gas burners” The 20th World Gas Conference Proceedings, Copenhagen.

Taylor, J. D., Allendorf, M. D., McDaniel, A. H., Rice S. F., 2003 “In situ diagnostics and modeling of methane catalytic partial oxidation on Pt in a stagnation-flow reactor”, Industrial & Engineering Chemistry Research, 42 (25): 6559-6566  
<http://dx.doi.org/10.1021/ie020934r>

Vlachos, D. G., 1996, “Homogeneous-heterogeneous oxidation reactions over platinum and inert surface”, Chemical Engineering Science, 51 (10):2429-2438  
[http://dx.doi.org/10.1016/0009-2509\(96\)00099-1](http://dx.doi.org/10.1016/0009-2509(96)00099-1)